



## Synthesis of Graphene Oxide as an Adsorbent for the Removal of Bisphenol A



Davoud Balarak <sup>a\*</sup> | Hossein Ansari <sup>a</sup> | Mahdethe Dashtizadeh <sup>b</sup> | Maryam Bazi <sup>b</sup>

<sup>a</sup> Department of Environmental Health, Health Promotion Research Center, Zahedan University of Medical Sciences, Zahedan, Iran.

<sup>b</sup> Department of Environmental Health, Student Research Committee, Zahedan University of Medical Sciences, Zahedan, Iran.

### \*Corresponding author: Davoud Balarak

Department of Environmental Health, Health Promotion Research Center, Zahedan University of Medical Sciences, Zahedan, Iran. Postal code: 35175-19111.

**E-mail address:** [dbalarak2@gmail.com](mailto:dbalarak2@gmail.com)

### ARTICLE INFO

#### Article type:

Original article

#### Article history:

Received: 16 June 2019

Revised: 12 August 2019

Accepted: 4 September 2019

DOI: [10.29252/jhehp.5.3.1](https://doi.org/10.29252/jhehp.5.3.1)

#### Keywords:

Graphene oxide

Adsorption

Kinetics

Bisphenol A

### ABSTRACT

**Background:** Phenolic compounds are an important group of pollutants in industrial wastewater, which must be treated before disposal into water resources. The present study aimed to use synthesized graphene oxide (SGO) to remove bisphenol A (BPA) from aqueous solutions.

**Methods:** Graphene oxide was synthesized using Hummers' method, and BPA adsorption was assessed as a function of solution pH, contact time, adsorbent dosage, and initial BPA concentration using the batch method. Isotherms and kinetic evaluation of dye adsorption was performed using the equilibrium data.

**Results:** Adsorption was rapid and strongly dependent on pH and adsorbent dosage, reaching the peak at the pH of 7 and adsorbent dosage of 0.8 g/l. BPA removal efficiency at the initial concentration of 10 mg/l was  $98.8 \pm 0.62\%$ . Analysis of the experimental isotherm data using the Langmuir-Freundlich and Temkin models indicated that the removal process followed the Langmuir isotherm, while the adsorption kinetics followed the pseudo-second-order kinetic model. The maximum adsorption capacity was calculated by Langmuir fitting and determined to be  $58.12 \pm 1.14$  mg/g.

**Conclusion:** According to the results, SGO could be employed as an effective agent for the removal of BPA from aqueous solutions.

## 1. Introduction

Disposal of wastewater into the environment is a major source of environmental pollution [1]. There are growing concerns regarding the widespread contamination of surface water and groundwater sources by various organic compounds due to the rapid development of chemical and petrochemical industries over the past decades [2,3]. Phenolic compounds commonly enter aqueous effluents as a result of various manufacturing processes, such as oil refinement, coke plants, adhesives, and polyamide and phenolic resin plants [4,5]. Bisphenol A (BPA) is a chemical that disrupts the endocrine function and has estrogenic

activity, interfering with the reproductive system of animals and humans even at low concentrations [6,7]. BPA is an antioxidant, which is non-biodegradable and highly resistant to chemical degradation, so that its high concentrations could be found in surface water and industrial wastewater [8,9]. BPA is released into the environment during various manufacturing processes and through leaching from final products [10,11].

Complete removal of phenolic compounds has not been achieved through biological processes in conventional wastewater treatment plants due to their complex molecular structures and low biodegradability [12,13].

**How to cite:** Balarak D, Ansari H, Dashtizadeh M, Bazi M. Synthesis of Graphene Oxide as an Adsorbent for the Removal of Bisphenol A. *J Hum Environ Health Promot.* 2019; 5(3): 98-103.



Therefore, advanced treatments are required for the effective elimination of phenolic compounds from various water sources [14].

The treatment of these effluents is essential prior to their discharge into the environment. Several methods have been proposed for the removal of phenolic compounds from effluents, including biological treatment, chemical oxidation, membrane processes, photochemical processes, ozonation, adsorption onto activated carbon, chemical treatment methods, and electrochemical processes (e.g., electrocoagulation) [15, 16].

In general, adsorption and advanced chemical oxidation are used for the advanced removal of phenolic compounds [17]. In these methods, adsorption is considered superior in terms of the initial costs, ease of operation, and no possibility of producing harmful secondary substances [18,19]. Among these treatment techniques, physical adsorption is considered to be most efficient in the rapid removal of BPA from effluents with several advantages over the other techniques, including relatively lower operating costs, ease of operation, and production of fewer secondary products [20,21].

Graphene is a novel, two-dimensional carbon nanomaterial, which is a fundamental building block for buckyballs, carbon nanotubes, and graphite. This substance has attracted the attention of scientists in recent years [22]. Graphene oxide (GO) is a precursor for graphene preparation, which is obtained through the strong oxidation of graphite using the modified Hummers' method [23]. Large quantities of oxygen atoms are found on the surface of the resulting GO in the form of epoxy, hydroxyl, and carboxyl groups. The presence of these functional groups on GO makes this substance extremely hydrophilic, providing the capability to apply GO in aquatic and biological environments [22,23].

The present study aimed to investigate the capability of synthesized graphene oxide (SGO) as an adsorbent in the removal of BPA from wastewater and assess the effects of the initial BPA concentration, adsorbent dosage, pH, and contact time on the adsorption process in order to determine the optimal conditions.

## 2. Materials and Methods

All the chemicals used in the study were of the analytical reagent grade and applied without further purification. BPA was obtained from Merck, Germany and used without further purification. BPA stock solutions were prepared by dissolving accurately weighted BPA in distilled water to the concentration of 1,000 mg/l, and the concentrations of the experimental solutions were achieved through dilution.

GO was synthesized from graphite powder using the modified Hummers' method [22]. The GO solution was centrifuged at 12,000 rpm for 10 minutes, and the residues were collected for the absorption experiments. In addition, scanning electron microscopy (SEM) images were obtained using a field emission scanning electron microscope (model: JSM-7001F, Japan).

### 2.1. Batch BPA Adsorption Experiments

The adsorption experiments were performed in the batch mode by shaking and adding the SGO concentrations to 50 milliliters of the BPA solution. For the kinetic studies, one

gram of SGO was added to 50 milliliters of the BPA solution at the concentration of 100 mg/l. Afterwards, adsorption was carried out in a flask containing the SGO and BPA solution at room temperature with the initial pH and constant agitation (100 rpm). The concentration of BPA in the solution was analyzed at 10-120-minutes intervals after the separation of the solids by filtration.

For isotherm studies, one gram of the SGO and BPA solution at the initial concentration of 10-100 mg/l were combined in a shaker at 100 rpm at the initial temperature and pH for 90 minutes. The concentration of BPA in the solution was analyzed after the separation of the solids by filtration. Moreover, the concentration of BPA in the residual solutions was analyzed using a UV spectrometer (model: DR 5000) at the maximum wavelength ( $\lambda = 280$  nm), and the concentration of BPA was analyzed at the maximum wavelength. All the experiments were performed in duplicate, and the mean data were reported.

Adsorption capacity was calculated based on the mass balance of BPA in the solutions and expressed in the milligram units of BPA per gram of the adsorbent. The adsorption capacity at the equilibrium was calculated using equation 1, as follows [24]:

$$q_e = \frac{(C_0 - C_e)V}{m} \quad (1)$$

Where  $q_e$  and  $C_e$  are the BPA amount adsorbed per unit weight of the sorbent (mg/g) and the equilibrium concentration of BPA in the solution (mg/l), respectively,  $C_0$  shows the initial concentration of BPA (mg/l), and  $V$  and  $m$  represent the volume of the BPA solution (l) and mass of the applied adsorbent (g), respectively.

## 3. Results and Discussion

Figure 1 shows the SEM image of the prepared SGO. As can be seen, the SGO was partially transparent with some crumples and had lateral dimensions of several micrometers, with the small holes caused by overexposure to sonication. In addition, it suggested that the SGO nanosheets could be prepared successfully [22].

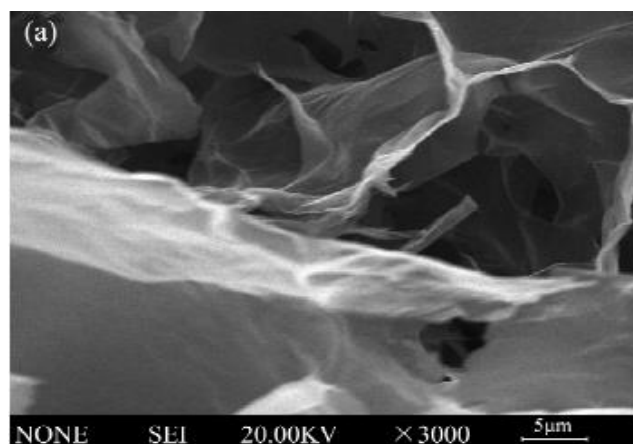


Figure 1: SEM image of SGO

### 3.1. Effect of the Contact Time

As was observed in all the initial BPA concentrations, the adsorption process could be divided into two phases (Figure

2). The first rapid phase passed within the first 45 minutes, followed by the second slower phase until reaching the equilibrium at 90 minutes. The rapid phase was due to the availability of adequate free active binding sites on the adsorbent surface [25]. During the second phase, the number of the free binding sites decreased, and the competition among the BPA also led to the reduction of the adsorption rate and effectiveness [18]. In a similar study conducted by Balarak et al. (2016) [16] regarding the efficiency of barley husk in the removal of BPA, the equilibrium time was determined to be 90 minutes.

### 3.2. Effect of the Adsorbent Dosage

Figure 3 depicts the effect of the adsorbent dosage on the adsorption of BPA from the aqueous solution onto the SGO. Accordingly, the increase dosage of the adsorbent was associated with the higher removal rate, which was attributed to the increased number of the active sites available for the binding of BPA at higher SGO dosages. Furthermore, a reverse trend was observed, in which the adsorption uptake capacity decreased at higher adsorbent concentrations [26]. The reduction could be due to the higher SGO dosage, which provided more active sites and caused the adsorption sites to remain unsaturated during the adsorption process [19]. In a study conducted by Gong et al. (2016) increased adsorbent dosage was reported to increase the removal efficiency due to the higher number of the available active sites [15].

### 3.3. Effect of pH

In the current research, the effect of pH on the adsorption of BPA onto SGO was assessed with the initial BPA concentration, SGO dosage, and contact time fixed at 25 mg/l, 0.8 g/l, and 90 minutes, respectively. Figure 4 shows the effect of pH on the adsorption of BPA. According to the findings, the highest adsorption capacity of the SGO was obtained at the pH of 7 (30.25 mg/g). In addition, the adsorption capacity significantly decreased at acidic and basic pH values. Similar results have been proposed in the literature regarding the adsorption of BPA onto activated carbon [4]. At acidic and basic pH values, H<sup>+</sup> and OH<sup>-</sup> may occupy the adsorption sites of the SGO [4], while low adsorption capacities at low and high pH values may occur due to the competitive adsorption between the H<sup>+</sup> and OH<sup>-</sup> ions and BPA molecules [6].

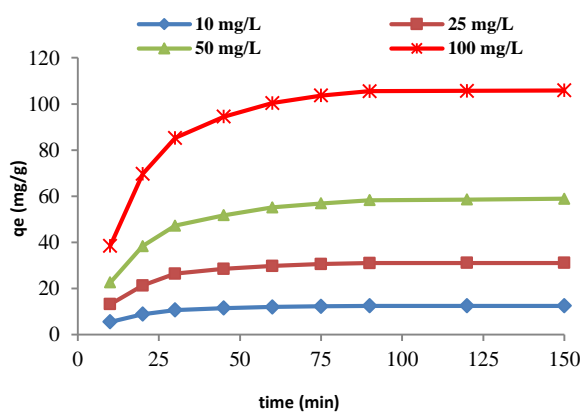


Figure 2: Effect of Contact Time and Initial BPA Concentration on BPA Removal Efficiency (pH = 7, adsorbent dosage = 0.8 g/l)

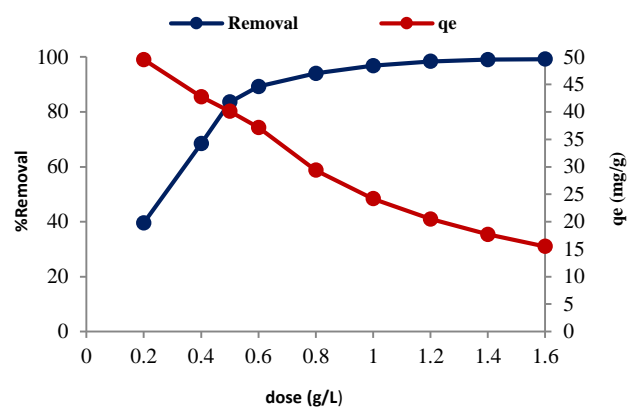


Figure 3: Effect of Adsorbent Dosage on BPA Removal Efficiency (contact time: 90 min, C<sub>0</sub> = 25 mg/l, pH = 7)

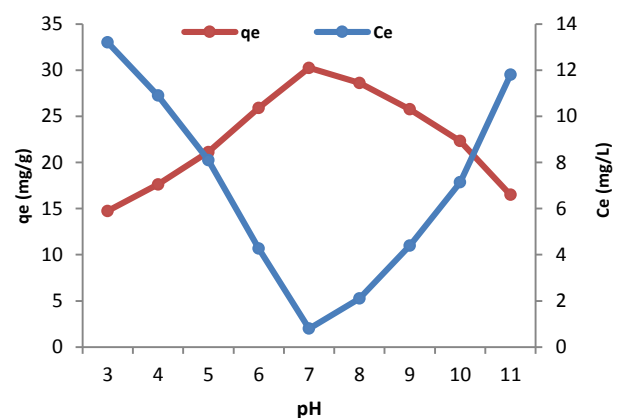


Figure 4: Effect of pH on BPA Removal Efficiency (C<sub>0</sub> = 25 mg/l, contact time: 90 min, adsorbent dosage = 0.8 g/l)

### 3.4. Effects of the Initial Concentration of PBA and Adsorption Kinetics

Adsorption kinetics governs the reaction rate, which determines the residence time and is an important characteristic defining the efficiency of an adsorbent. In the present study, the pseudo-first-order, pseudo-second-order, and intraparticle diffusion kinetic models were applied to the experimental data, and their kinetic parameters are presented in table 1.

Based on the Lagergren pseudo-first-order model, the occupation rate of adsorption sites is proportional to the number of the unoccupied sites, and the linear form of the model equation is as follows [24]:

$$\log (q_e - q_t) = \log q_e - \frac{K_1}{2.303} t \tag{2}$$

Where K<sub>1</sub> is the Lagergren rate constant of adsorption (min<sup>-1</sup>), and q<sub>e</sub> and q<sub>t</sub> represent the amount of adsorbed BPA (mg/g) at the equilibrium and time, respectively. In the current research, the slope and intercept of the plots of log (q<sub>e</sub>-q<sub>t</sub>) versus t were used to determine the pseudo-first-order rate constant K<sub>1</sub> and the equilibrium adsorption capacity q<sub>e</sub> for BPA.

The pseudo-second-order model is based on the assumption that adsorption follows a second-order mechanism. Therefore, the occupation rate of the

adsorption sites is proportional to the square of the number of the unoccupied sites. The linear form of the pseudo-second-order equation was expressed, as follows [25]:

$$\frac{t}{q_t} = \frac{1}{k_2 q_e^2} + \frac{1}{q_e} t \tag{3}$$

Where  $K_2$  (g/mg.min) is the equilibrium constant of the pseudo-second-order adsorption. The applicability of the pseudo-second-order model was evaluated using the linear plot of  $t/q_t$  versus  $t$  (Figure 5), with the slope of  $1/q_e$ , and the  $K_2$  value was calculated based on the plot intercept. In addition, the diffusion mechanism was determined using the intraparticle diffusion model due to the fact that the BPA ions were transported from the aqueous phase to the surface of the adsorbent, thereby diffusing into the interior of the particles if they were porous. The intraparticle diffusion equation was as follows [26]:

$$q_t = k_d t^{0.5} + C \tag{4}$$

Where  $C$  is the intercept, and  $K_d$  (mg/gmin<sup>1/2</sup>) denotes the intraparticle diffusion rate constant. Intraparticle diffusion is the sole rate determining the whether the plot of  $q_t$  versus  $t^{1/2}$  is linear and passes through the origin. The values of  $q_t$  and  $C$  were obtained based on the slope and intercept of the plot (Table 1).

based on the slope and intercept of the plot (Table 1).

Comparison of the correlation-coefficient results (Table 1) indicated that both the pseudo-first-order and pseudo-second-order models provided good fits to the experimental data on BPA. However, the  $R^2$  values presented by the pseudo-second-order model were superior to the pseudo-first-order model, which indicated the greater conformity of the adsorption process to the former. Furthermore, the calculated  $q_e$  values ( $q_e$  cal), which were obtained from the pseudo-first-order model, demonstrated showed great discrepancy with the experimental  $q_e$  value ( $q_e$  exp) for the adsorption of BPA unlike the pseudo-second-order model.

In the investigation of the diffusion mechanism, the  $R^2$  values obtained from the intraparticle diffusion model exhibited proper correlation, which indicated the presence of the intraparticle diffusion mechanism in the adsorption of BPA onto the SGO although it was not the sole rate determining step due to the occurrence of the intercept. Moreover, the plot intercept reflected the boundary layer effect, and larger intercept was associated with the greater contribution of the surface sorption to the rate determining step.

### 3.5. Adsorption Isotherm Models

The adsorption isotherm was conducted at the equilibrium for the removal of BPA from an aqueous solution in order to obtain a correlation between the quantity of the BPA adsorbed onto the GO, retaining in the aqueous solution. In this regard, the experimental data of the present study were fitted to three different isotherm models.

The Langmuir adsorption model is based on monolayer adsorption, where adsorption exclusively occurs at definite sites that are fixed in terms of the number and equivalence and are identical. The Langmuir equilibrium adsorption equation is as follows [27]:

$$q_e = \frac{q_{max} b C_e}{1 + b C_e} \tag{5}$$

Where  $q_e$  is the equilibrium adsorption capacity of the adsorbent (mg/g),  $q_{max}$  denotes the maximum adsorption capacity (mg/g),  $C_e$  shows the equilibrium concentration (mg/l), and  $b$  is the Langmuir constant (l/mg) representing the degree of the adsorption affinity of the adsorbate. As such, higher  $b$  value is associated with the stronger affinity of the ion toward the adsorbent.

equation 6 could be used as a linear form, as follows [25]:

$$\frac{C_e}{q_e} = \frac{1}{q_{max}} C_e + \frac{1}{b q_{max}} \tag{6}$$

Where  $R_L$  is a dimensionless constant known as the separation factor or equilibrium parameter and represented, as follows [28]:

$$R_L = \frac{1}{1 + b C_0} \tag{7}$$

This parameter determined whether the isotherm is favorable ( $R_L < 1$ ), unfavorable ( $R_L > 1$ ), irreversible ( $R_L = 0$ ) or linear ( $R_L = 1$ ).

The Freundlich model is the first expression to describe multilayer adsorption, and the Freundlich isotherm is an empirical equation employed to describe heterogeneous systems and is expressed, as follows [29]:

$$q_e = K_f C_e^{1/n} \quad n > 1 \tag{8}$$

The linearized Freundlich isotherm equation could also be expressed, as follows [14]:

$$\ln q_e = \ln K_f + \frac{1}{n} \ln C_e \tag{9}$$

Where  $n$  and  $K_f$  are the Freundlich constants for the intensity and capacity of adsorption, respectively. Based on the slope and intercept of the linear plot for the experimental data  $\ln q_e$  versus  $\ln C_e$ , the  $n$  and  $K_f$  values could can be calculated. In this equation,  $(1/n)$  is the slope, and  $\ln K_f$  is the intercept. In addition, the slope with the range of zero and unity is an indication of the heterogeneity of the surface and intensity of adsorption as the slope is extremely low (near zero), while a slope near unity refers to the chemisorption process, where  $1/n$  is higher than unity, implying cooperative adsorption [21].

The Temkin model assumes the uniform distribution of the surface binding energy, and for all the molecules, the adsorption heat decreases linearly with the increased adsorbent surface coverage. This model could be expressed, as follows[19]:

$$q_e = \frac{RT}{b_T} \ln A_T C_e \tag{10}$$

Where  $A_T$  is the binding constant of the equilibrium (l/g) identical to the extreme binding energy,  $b_T$  is the Temkin isotherm constant regarding the adsorption heat (J/mol),  $R$  shows the universal gas constant (8.314 J/mol K), and  $T$  represents the absolute temperature (K). Therefore, equation 11 could be proposed in the linear form, as follows [30]:

**Table 1:** Kinetic parameters for the adsorption of BPA onto SGO at various concentration

C <sub>0</sub> (mg/L)	q <sub>e(exp)</sub> (mg/g)	Pseudo-first order			Pseudo-second order			Intraparticle diffusion		
		K <sub>1</sub>	q <sub>e</sub> (mg/g)	R <sup>2</sup>	K <sub>2</sub>	q <sub>e</sub> (mg/g)	R <sup>2</sup>	K <sub>p</sub>	C	R <sup>2</sup>
10	12.47	0.0591	6.418	0.842	0.0087	11.44	0.996	0.278	2.761	0.912
25	31.03	0.0472	14.96	0.859	0.0065	27.36	0.998	0.341	3.925	0.881
50	58.86	0.0419	25.34	0.882	0.0051	52.73	0.999	0.409	5.411	0.873
100	105.68	0.0283	57.91	0.893	0.0047	102.82	0.997	0.457	6.842	0.854

**Table 2:** Isotherms constants for the removal BPA onto SGO

Langmuir model					Freundlich model			Temkin model		
q <sub>m</sub>	R <sub>L</sub>	b	R <sup>2</sup>	n	K <sub>F</sub>	R <sup>2</sup>	A <sub>T</sub>	b <sub>T</sub>	R <sup>2</sup>	
58.12	0.272	0.518	0.996	4.11	0.921	0.886	0.849	24.61	0.862	

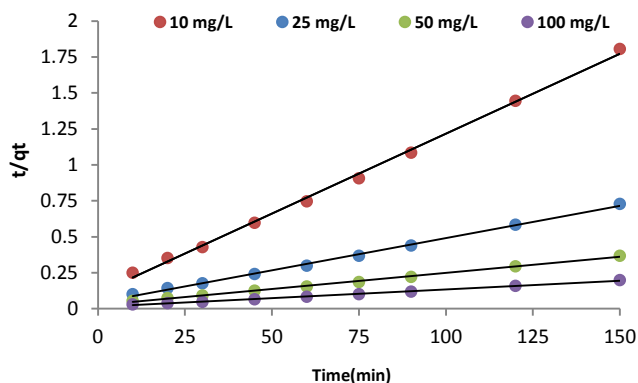


**Figure 5:** Pseudo-second-order Kinetic Plots for BPA Adsorption onto SGO

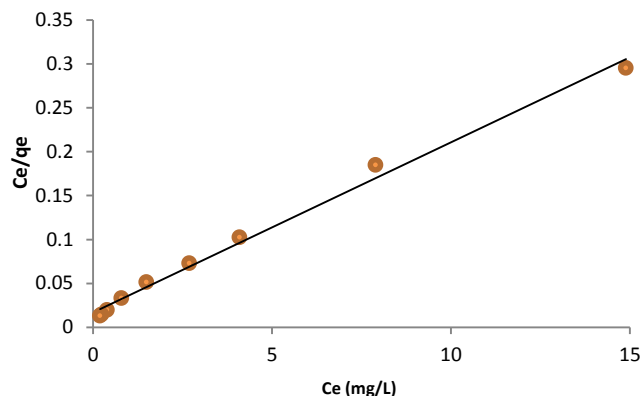


**Figure 6:** Langmuir Plots for Adsorption of BPA onto SGO

$$q_e = \frac{RT}{b_T} \ln A_T + \frac{RT}{b_T} \ln C_e \tag{11}$$

Where A<sub>T</sub> and b<sub>T</sub> show the isotherm constants, which could be evaluated from the plot of q<sub>e</sub> versus ln C<sub>e</sub>.

The experimental data were fitted to three linearized isotherm models (Langmuir, Freundlich, and Temkin). For these models, the obtained parameters and the regression correlation coefficient (R<sup>2</sup>) are listed in table 2. It is clear from table 2 that Langmuir isotherm model plot (Figure 6) has the best fitting for the adsorption of BPA on SGO (R<sup>2</sup> = 0.996). Therefore, the adsorption process can be described by the formation of monolayer coverage of the adsorbate on the homogeneous adsorbent surface. The calculated maximum adsorption capacity (q<sub>max</sub>) of SGO was found to be closer to the experimental value (58.12 mg/g).

#### 4. Conclusion

This study aimed to investigate the adsorption efficiency of SGO in the removal of BPA from aqueous solutions through the batch process. According to the results, the removal of BPA by the SGO depended on the contact time and adsorbent dosage. On the other hand, the adsorption process was observed to be rapid, and the equilibrium was achieved within 90 minutes. In addition, increased adsorbent dosage was associated with the higher removal efficiency of BPA by the adsorbent. The applicability of the pseudo-first-order, pseudo-second-order, and intraparticle diffusion models was also investigated, and the experimental data were better correlated with the pseudo-second-order model compared to the other models.

#### Authors' Contributions

D.B., designed the interview forms for all the sectors with the cooperation of M.D., who conducted the interviews; H.A., analyzed the data and drafted the manuscript; M.B., conducted the research and revised the manuscript.

#### Conflict of Interest

The Authors declare that there is no conflict of interest.

#### Acknowledgments

Hereby, we extend our gratitude to Zahedan University of Medical Sciences for the financial support of this research project (Project No. 9462).

#### References

- Assadi A, Soudavari A, Mohammadian M. Comparison of Electrocoagulation and Chemical Coagulation Processes in Removing Reactive red 196 from Aqueous Solution. *J Hum Environ Health Promot.* 2016; 1(3): 172-82.
- Soni H, Padmaja P. Palm Shell Based Activated Carbon for Removal of Bisphenol A: An Equilibrium, Kinetic and Thermodynamic Study. *J Porous Mater.* 2014; 21: 275-84.
- Yu JG, Zhao XH, Yang H, Chen XH, Yang Q, Yu LY, et al. Aqueous Adsorption and Removal of Organic Contaminants by Carbon Nanotubes. *Sci Total Environ.* 2014; 482: 241-51.
- Liu G, Ma J, Li X, Qin Q. Adsorption of Bisphenol A from Aqueous Solution onto Activated Carbons with Different Modifications Treatments. *J Hazard Mater.* 2009; 164: 1275-80.
- Zheng S, Sun Z, Park Y, Ayoko GA, Frost RL. Removal of Bisphenol A from

- Wastewater by Camontmorillonite Modified with Selected Surfactants. *Chem Eng J.* 2013; 234: 416-22.
- Bautista Toledo I, Ferro Garcia MA, Rivera Utrilla J, Moreno Castilla C, Vegas Fernández FJ. Bisphenol A Removal From Water by Activated Carbon. Effects of Carbon Characteristics and Solution Chemistry. *Environ Sci Technol.* 2005; 36: 6246-50.
  - Dong Y, Wu D, Chen X, Lin Y. Adsorption of Bisphenol A from Water by Surfactant-Modified Zeolite. *J Colloid Interface Sci.* 2010; 348: 585-90.
  - Pan J, Yao H, Li X, Wang B, Huo P, Xu W, et al. Synthesis of Chitosan/ $\gamma$ - $\text{Fe}_2\text{O}_3$ /fly-ash-Cenospheres Composites for the Fast removal of Bisphenol A and 2, 4, 6-Trichlorophenol from Aqueous Solution. *J Hazard Mater.* 2011; 190: 276-84.
  - İpek İY, Yüksel S, Kabay N, Yüksel M. Investigation of Process Parameters for Removal of Bisphenol A (BPA) from Water by Polymeric Adsorbents in Adsorption-Ultrafiltration Hybrid System. *J Chem Technol Biotechnol.* 2014; 89: 835-40.
  - Laatikainen K, Bryjak M, Laatikainen M. Molecularly Imprinted Poly Styrenedivinyl Benzene Adsorbents for Removal of Bisphenol A. *Desalination Water Treat.* 2014; 52: 1885-94.
  - Yamamoto T, Yasuhara A, Shiraishi H, Nakasugi O. Bisphenol A in Hazardous Waste Landfill Leachates. *Chemosphere.* 2001; 42: 415-8.
  - Balarak D, Mostafapour FK, Lee SM, Jeon C. Adsorption of Bisphenol A Using Dried Rice Husk: Equilibrium, Kinetic and Thermodynamic Studies. *Appl Chem Eng.* 2019; 30(3): 316-23.
  - Seyhi B, Drogui P, Buelna G, Blais JF. Modeling of Sorption of Bisphenol A in Sludge Obtained from a Membrane Bioreactor Process. *Chem Eng J.* 2011; 172: 61-7.
  - Guo W, Hu W, Pan J, Zhou H, Guan W, Wang X, et al. Selective Adsorption and Separation of BPA from Aqueous Solution Using Novel Molecularly Imprinted Polymers Based on Kaolinite/ $\text{Fe}_3\text{O}_4$  Composites. *Chem Eng J.* 2011; 171: 603-11.
  - Gong R, Jiang Y, Cai W, Zhang K, Yuan B, Jiang J. Enhanced Sorption of Bisphenol A on  $\alpha$ -Ketoglutaric Acid-Modified Chitosan Resins by Hydrophobic Sorption of Hemimicelles. *Desalination.* 2010; 258(1-3): 54-8.
  - Balarak D. Kinetics, Isotherm and Thermodynamics Studies on Bisphenol A Adsorption Using Barley Husk. *Int J Chemtech Res.* 2016; 9(5): 681-90.
  - Zhou Y, Chen L, Lu P, Tang X, Lu J. Removal of Bisphenol A from Aqueous Solution Using Modified Fibric Peat as a Novel Biosorbent. *Sep Purif Technol.* 2011; 81: 184-90.
  - Tsai WT, Lai CW, Su TY. Adsorption of Bisphenol-A from Aqueous Solution onto Minerals and Carbon Adsorbents. *J Hazard Mater.* 2006; 134: 169-75.
  - Namasivayam C, Sumithra S. Adsorptive Removal of Phenols by Fe(III)/Cr(III) Hydroxide and Industrial Solid Waste. *Clean Technol Environ Policy.* 2007; 9: 215-23.
  - Zazouli MA, Mahdavi Y, Bazrafshan E, Balarak D. Photodegradation Potential of Bisphenol A from Aqueous Solution by *Azolla Filiculoides*. *J Environ Health Sci Eng.* 2014; 12(1): 66-74.
  - Zaib Q, Khan IA, Saleh NB, Flora JR, Park YG, Yoon Y. Removal of Bisphenol A and 17 $\beta$ -Estradiol by Single-Walled Carbon Nanotubes in Aqueous Solution: Adsorption and Molecular Modeling. *Water Air Soil Pollut.* 2012; 223(6): 3281-93.
  - Tazerodi A J, Akbari H, Mostafapour F. Adsorption of Catechol from Aqueous Solutions Using Graphene Oxide. *J Hum Environ Health Promot.* 2018; 4 (4): 175-9.
  - Yang ST, Chen S, Chang Y, Cao A, Liu Y, Wang H. Removal of Methylene Blue from Aqueous Solution by Graphene Oxide. *J Colloid Interface Sci.* 2011; 359(1): 24-9.
  - Zhao Z, Fu D, Ma Q. Adsorption Characteristics of Bisphenol A from Aqueous Solution onto Hdtmab-Modified Palygorskite. *Sep Sci Technol.* 2014; 49(1): 81-9.
  - Park Y, Sun Z, Ayoko GA, Frost RL. Bisphenol A Sorption by Organo-Montmorillonite: Implications for the Removal of Organic Contaminants from Water. *Chemosphere.* 2014;107: 249-56.
  - Balarak D, Mahdavi Y, Kord Mostafapour F, Joghataei A. Batch Removal of Acid Blue 292 Dye by Biosorption onto *Lemna minor*: Equilibrium and Kinetic Studies. *J Hum Environ Health Promot.* 2016; 2(1): 9-19.
  - Moussavi SP, Mohammadian Fazli M. Acid Violet 17 Dye Decolorization by Multi-Walled Carbon Nanotubes from Aqueous Solution. *J Hum Environ Health Promot.* 2016; 1(2): 110-7.
  - Balarak D, Dashtizadeh M, Zafariyan M, Sadeghi M. Equilibrium, Isotherm and Kinetic Adsorption Studies of Direct Blue 71 onto Raw Kaolin. *J Hum Environ Health Promot.* 2018; 4 (4): 153-8.
  - Srivastava VC, Swamy MM, Mall ID, Prasad B, Mishra IM. Adsorptive Removal of Phenol by Bagasse Fly Ash and Activated Carbon: Equilibrium, Kinetics and Thermodynamics. *Colloids Surf A Physicochem Eng Asp.* 2006; 272(1-2): 89-104.
  - Balarak D, Dashtizadeh M, Abasizade H, Baniasadi M. Isotherm and Kinetic Evaluation of Acid Blue 80 Dye Adsorption on Surfactant-Modified Bentonite. *J Hum Environ Health Promot.* 2018; 4 (2): 75-80.